Applying the Rayleigh approach for stable isotope-based analysis of VOC biodegradation in diffusion-dominated systems

Ali M. Khan, Lukas Y. Wick, Martin Thullner[*]

Department of Environmental Microbiology, UFZ - Helmholtz Centre for Environmental Research,

Leipzig, Germany

[*] Corresponding author: Mailing address: Helmholtz Centre for Environmental Research - UFZ. Department of Environmental Microbiology; Permoserstrasse 15; 04318 Leipzig, Germany. phone: +49 341 235 1338, fax: +49 341 235 451338, e-mail: martin.thullner@ufz.de.

ABSTRACT

Compound-specific stable isotope analysis (CSIA) has become an established tool for assessing biodegradation in the subsurface. Diffusion-dominated vapor phase transport thereby is often excluded from quantitative assessments due to the problem of diffusive mixing of concentrations with different isotopic signatures for CSIA interpretation. In soils and other unsaturated porous media volatile organic compounds (VOCs) however are mainly transported via gas-phase diffusion and may thus prohibit a CSIA-based quantitative assessment of the fate of VOC. The present study presents and verifies a concept for the assessment of biodegradation-induced stable isotope fractionation along a diffusive transport path of VOCs in unsaturated porous media. For this purpose data from batch and column toluene biodegradation experiments in unsaturated porous media were combined with numerical reactive transport simulations; both addressing changes of concentration and stable isotope fractionation of toluene. The numerical simulations are in good agreement with the experiment data, and our results show that the presented analytically derived assessment concept allows using the slope of the Rayleigh plot to obtain reasonable estimates of effective *in-situ* fractionation factors in spite of diffusion-dominated transport. This enlarges the application range of CSIA and provides a mean for a better understanding of VOC fate in the unsaturated subsurface.
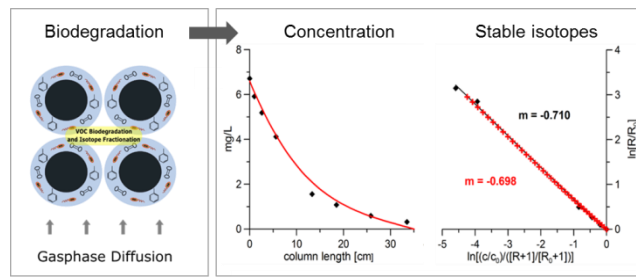
Keywords: Volatile organic compounds (VOC), Subsurface processes, Reactive transport modeling, Compound-specific stable isotope analysis (CSIA), Biodegradation, Bioremediation, Unsaturated zone, Outgasing.

52 **TOC**

53

Biodegradation → Concentration · Stable isotopes

Gasphase Diffusion

m = -0.710

m = -0.698

54

55

INTRODUCTION

Biodegradation of volatile organic compounds (VOCs) in the unsaturated subsurface has been observed for different laboratory and field conditions,[1-4] indicating that natural attenuation may be a feasible remediation option for VOCs in the unsaturated subsurface. However, the fate of subsurface vapor-phase VOCs depends on a multitude of hydrological, geochemical, and microbiological processes. These processes are not only highly interlinked and dependent on temperature, water saturation, pH and many other environmental factors, but also act in parallel, making the *in-situ* identification and quantification of the key processes controlling the system dynamics difficult. In order to distinguish biodegradation from other processes, Compound-Specific Stable Isotope Analysis (CSIA) is widely accepted as a monitoring strategy and as a powerful tool in studying the fate and behavior of contaminants in groundwater systems.[5-8] The application of CSIA makes use of the fact that the stable isotope fractionation of the biodegradation reaction dominates the change of the stable isotope signature of the contaminants. Especially for a quantitative analysis of biodegradation using CSIA, it is required that contributions from mixing,[8-10] sorption,[11-13] small-scale mass transfer,[14-15] dispersion[8, 16-18] or the regeneration of a degraded compound[19] can be either neglected or their influence be adequately considered. If these assumptions are met, the analytical Rayleigh model[20-21] is frequently used to deduce the extent of biodegradation from the degree of isotopic enrichment[22-23] in groundwater systems with advection-dominated transport.

In the gas phase, molecular diffusion coefficients are up to four orders of magnitude larger than in the aqueous phase. Thus - in contrast to groundwater systems - transport in the gas phase of the unsaturated subsurface is more easily dominated by diffusion in the absence of relevant pressure gradients. As diffusion coefficients in the gas phase[24-25] as well as the aqueous phase[26-28] can differ between isotopologues (i.e. between chemically identical species with different isotopic composition), diffusion-dominated transport systems may exhibit significant stable isotope fractionation even in the absence of biodegradation.[27, 29-31] Furthermore, even if diffusive transport is not leading to any fractionation effects, diffusive mixing along concentration gradients mitigates changes in stable isotope signatures caused by biodegradation. As a consequence it has

been considered that the standard Rayleigh-equation based analysis approach of stable isotope fractionation is not applicable for diffusion-dominated transport systems.[29] This would mean that for diffusion-dominated transport systems CSIA could at best be used as qualitative biodegradation indicator only. However, for the related case of soil organic matter decomposition quantitative assessment approaches could be obtained describing the fractionation of CO_2 as volatile reaction product in spite of the diffusion dominated transport regime.[25, 32]

The aim of this study is to show that even for diffusion dominated sytems CSIA data might still be used to obtain a quantitative understanding of VOC biodegradation. For this we use experimental results published in Khan, et al.[4] showing efficient biodegradation in a column reactor systems mimicking the conditions in the unsaturated subsurface above the groundwater table. Data form the column reactors and additional batch experiments are analyzed regarding stable isotope fractionation and interpreted using a combination of analytical calculations and numerical modeling. To address the complex interplay of processes and their impact on the fate of bioreactive species in the subsurface, numerical reactive transport models are powerful means[33] and have shown their potential also for the analysis of VOC biodegradation in unsaturated systems.[34-35] In recent years, reactive transport modeling concepts have been expanded to consider isotope-specific processes and the resulting stable isotope fractionation.[1, 15, 36-44] This provides an approach to disentangle the potential influence of different processes on stable isotope fractionation effects experimentally observed in subsurface compartments.

In this study a combination of simplified analytical calculations with numerical reactive transport simulations is used to determine to which extent the simplified calculations lead to acceptable estimates of the fractionation effects observed experimentally and to show that also for diffusion-dominated transport system a quantitative analysis of CSIA can be obtained via a modified interpretation of the analytical Rayleigh model.

MATERIALS & METHODS

Batch Reactors

Batch reactor systems were used to quantify stable hydrogen isotope fractionation factors during biodegradation of vapor-phase toluene. Gastight chromoflax glass bottles with total volume of 1150 mL were used as batch reactors (**SI, Figure S1**). Reactors were filled with 50 mL glass beads (d = 2.9 – 3.5 mm), coated with minimal media agar that contained toluene degrading bacteria (Pseudomonas putida KT2442 DsRed pWW0 gfp) at a density of 3.95 x 10^8 cfu per gram of glass beads as previously described by Khan, et al.[4] The minimal medium agar layer contained all nutrients relevant for bacterial activity and growth.[45] The headspace of the batch reactor (1100 mL) was provided sufficient oxygen (for bacterial activity during the entire experimental period. As sorption of nonionic, hydrophobic organic chemicals to mineral surfaces is expected to be negligible,[46] no controls assessing the adsorption of agar-born MTBE and toluene to glass were performed. Four different operation modes were applied each characterized by specific period of time (1 to 4 days) the reactors were first kept at room temperature under sterile conditions for 1 to 4 days before toluene was added. After this reactor-specific resting period, a known concentration of a 1:1 mixture of toluene and perdeuterated toluene was spiked to the internal glass wall close to the neck of the reactor. Methyl tert-butyl ether (MTBE) was additionally added as a non-reactive VOC control. This allowed us to get 20 mg L^{-1} total gas phase concentration of the two toluene isotopologues, and 5 mg L^{-1} gas phase concentration of MTBE.

After spiking of the VOCs, the batch reactors were let to equilibrate regarding volatilization for 20 minutes (allowing vapor-phase toluene concentrations to achieve calculated equilibrium values) before the start of sampling (marked as time $t_0 = 0$ hours). Subsequent samples were taken every hour until $t = 8$ hours. Gas-phase VOC samples were taken and analyzed as mentioned previously in Khan, et al. [4] (see also Supporting Information). The observation period was selected for the isotope analysis and the measured data (toluene concentration c and stable (hydrogen) isotope ratio R in the gas phase) were analyzed using Rayleigh plots (i.e., plotting the logarithmic form of the Rayleigh equation:[21, 47] *ln(R/R$_0$)* against *ln((c/c$_0$)/((R+1)/(R$_0$+1)))* for the large

149 values or R given here;[48] the subscript 0 refers to the initial conditions) to determine
150 stable isotope fractionation factors.

151

152 ***Column Reactors***

153 The column reactor experiments are described in detail in Khan, et al.[4] (see also
154 Supporting Information) and only a brief overview is given here: The setup consisted of
155 vertical chromoflax glass column reactors ($l = 35$ cm, *i.d.* = 4.1 cm) packed with agar-
156 coated 700 g glass beads ($d = 2.9–3.5$ mm), separated with 45 mL headspace from the
157 liquid reservoir of 2.375 L volume (**SI, Figure S2**). Column reactors were open to the
158 atmosphere on top to allow sufficient oxygen for biodegradation.[4] Known
159 concentrations of VOCs (toluene 37 mg L^{-1} and MTBE 20 mg L^{-1}) were spiked in the
160 liquid reservoirs with magnetic stirrer bars and were kept on magnetic shakers for 12
161 hours prior to the start of experiments to equilibrate. $HgCl_2$ (2 µg L^{-1}) was added to
162 avoid biodegradation in the liquid reservoirs. To avoid cross contamination the columns
163 were sterilized and were attached to the liquid reservoirs under sterile conditions.

164

165 Data were taken from two abiotic experiments ("Control 1" and "Control 2", termed
166 "Control" and "Control HC" in Khan, et al.[4]) as well as a set of three bioreactive
167 experiments ("Column 1", "Column 2" and "Column 3", termed "Bioreactor 1" to
168 "Bioreactor 3" in Khan, et al.[4]) where the glass bead packing was inoculated with
169 *Pseudomonas putida* KT2442 DsRed pWW0 gfp. Reactors were operated for 7 days at
170 standard pressure (1 atm) and T = 22 °C. Vapor-phase and liquid samples (500 µL)
171 were taken every day. To provide quasi steady-state conditions, an observation period
172 between day 2 and day 5 was selected for the evaluation of the vapor-phase results.

173

THEORETICAL APPROACHES

In this study, two different computational approaches are applied: an analytical approach relying on a simplified description of transport and degradation in the columns, and a numerical approach providing a more detailed description of the processes in the gas phase and in the aqueous phase of the combined reservoir-column system.

Analytical solutions for diffusive-reactive transport with first order degradation and stable isotope fractionation

The fractionation of stable isotopes by (bio-)reactive transformations is described by the isotope fractionation factor $\alpha_b = \dfrac{{}^h r / {}^h c}{{}^l r / {}^l c}$, where ${}^h r$ and ${}^l r$ are the reaction rates, and ${}^h c$ and ${}^l c$ are the gas phase concentrations of reactants containing the light or the heavy isotope, the latter denoted by the superscripts l and h, respectively. If the degradation reaction is following first order kinetics (${}^h r = {}^l k \cdot {}^l c$ and ${}^l r = {}^l k \cdot {}^l c$, with ${}^h k$ and ${}^l k$ as first order degradation rate parameters) this simplifies to $\alpha_b = \dfrac{{}^h k}{{}^l k}$. Analogously the stable isotope fractionation due to diffusive transport can be described by a factor $\alpha_d = \dfrac{{}^h D}{{}^l D}$, with ${}^{h,l} D$ as effective molecular diffusion coefficients.

If in a one-dimensional system diffusion and such degradation are the only processes acting on the concentration distribution of the compound, concentration changes are given as

$$\frac{\partial {}^{h,l} c}{\partial t} = {}^{h,l} D \cdot \frac{\partial^2 {}^{h,l} c}{\partial x^2} - {}^{h,l} k \cdot {}^{h,l} c \tag{1}$$

with and t and x as temporal and spatial coordinate, respectively.

For steady-state conditions ($\partial {}^{h,l} c / \partial t = 0$) and boundary condition of ${}^{h,l} c(x=0) = {}^{h,l} c_0$ and ${}^{h,l} c(x=L) = 0$ the solution of Eq. 1 is given by Wilson[49] and Pasteris, et al.[50]

$$ {}^{h,l} c(x) = {}^{h,l} c_0 \cdot \frac{\sinh\left(\sqrt{{}^{h,l} Da} \cdot \left(1 - \frac{x}{L} \right) \right)}{\sinh\left(\sqrt{{}^{h,l} Da} \right)} \tag{2}$$

with ${}^{h,l} Da = {}^{h,l} k \cdot L^2 / {}^{h,l} D$ as Damköhler number describing the ratio between the time scales of transport and of reaction.

201 In the case of L→∞ Eq. 2 simplifies to

$$^{h,l}c(x) = {}^{h,l}c_0 \cdot \exp\left(-\sqrt{\frac{^{h,l}k}{^{h,l}D}} \cdot x \right) \tag{3}$$

203 Using Eq. 3 the isotope ratio $R = {}^{h}c/c$ is given as

204 $$R = \frac{^{h}c_0 \cdot \exp\left(-\sqrt{\frac{^{h}k}{^{h}D}} \cdot x \right)}{^{l}c_0 \cdot \exp\left(-\sqrt{\frac{^{l}k}{^{l}D}} \cdot x \right)} = \frac{^{h}c_0 \cdot \exp\left(-\sqrt{\frac{\alpha_b}{\alpha_d}\frac{^{l}k}{^{l}D}} \cdot x \right)}{^{l}c_0 \cdot \exp\left(-\sqrt{\frac{^{l}k}{^{l}D}} \cdot x \right)}$$ which can be transformed into

205 $$\frac{R}{R_0} = \frac{\left({}^{l}c/{}^{l}c_0 \right)^{\sqrt{\alpha_b/\alpha_d}}}{\left({}^{l}c/{}^{l}c_0 \right)} = \left(\frac{^{l}c}{^{l}c_0} \right)^{\left(\sqrt{\alpha_b/\alpha_d} - 1 \right)} = \left(\frac{c/c_0}{(R+1)/(R_0+1)} \right)^{\left(\sqrt{\alpha_b/\alpha_d} - 1 \right)} \tag{4}$$

206 with $c = {}^{h}c + {}^{l}c$ and the subscript *0* denoting conditions at $x = 0$. Note that assuming c

207 $\approx {}^{l}c$ (i.e. $R \ll 1$) simplifies Eq. 4 to $\frac{R}{R_0} = \left(c/c_0 \right)^{\left(\sqrt{\alpha_b/\alpha_d} - 1 \right)}$. When plotting

208 concentration and isotope data in a Rayleigh plot (i.e., plotting the logarithmic form of

209 the Rayleigh equation: $ln(R/R_0)$ against $ln(c/c_0)$[21, 48]), the slope m of the Rayleigh plot

210 would thus be given by

211 $$m = \sqrt{\alpha_b/\alpha_d} - 1 \tag{5}$$

212 (and not by $m = \alpha_b - 1$ as predicted by the classical Rayleigh equation for advection

213 dominated transport or for batch systems). For other conditions, in particular for finite

214 size systems (finite L) and other than first order degradation kinetics, no closed form

215 analogue for Eq. 4 exists to our knowledge and it is not clear to which extent Eq. 5 can

216 be used as an approximate solution. Note that Eq. 5 is valid for systems with

217 biodegradation. In the absence of biodegradation no fractionation effects are present at

218 steady state.

219

220 *Numerical simulations*

221 The simulations of the column reactors presented in Khan, et al.[4] consider processes in

222 both parts of the reactors: the reservoir and the column. The reservoir is assumed to

223 contain a well-mixed liquid phase and a well-mixed gaseous head space. The exchange

224 of volatile compounds between these two phases is controlled by a linear exchange term

225 (Eq. 6). The column is spatially discretized along its length and is also assumed to

226 contain at each length a liquid and a gas phase using again a linear term for the

227 exchange of volatile compounds between the phases (Eq. 8). At the bottom of the

228 column concentration in the gas phase are coupled to those in the head space of the

229 reservoir using again such an exchange term (Eq. 7). Diffusive transport is assumed to

230 take place in the gas phase along the length of the column, no transport is considered

231 along the aqueous phase of the column. Biodegradation of toluene (i.e., $C_7H_8 + 9O_2 \rightarrow$

232 $7CO_2 + 4H_2O$) is restricted to the liquid phase of the first 30 cm of the column (from 30

233 to 35 cm the glass bead packing had not been inoculated in the experiments). Growth of

234 degrading microorganisms is not considered. To describe degradation and stable isotope

235 fractionation of toluene in the column reactors, deuterated and non-deuterated toluene

236 are simulated as individual species using Michaelis-Menten kinetics (isotope-specific

237 version adapted from Thullner, et al.[37]) for the degradation reaction (Eq. 9 and 10). This

238 results in the flowing set of expressions for the kinetics of the individual processes.

239 $$^{h,l}r_1 = {}^{h,l}k_1 \cdot \left({}^{h,l}c_{r,g} - {}^{h,l}c_{r,a} \cdot {}^{h,l}H \right) \text{ (phase exchange reservoir)} \tag{6}$$

240 $$^{h,l}r_2 = {}^{h,l}k_2 \cdot \left({}^{h,l}c_{x=0,g} - {}^{h,l}c_{r,g} \right) \quad \text{(exchange head space – column)} \tag{7}$$

241 $$^{h,l}r_3 = {}^{h,l}k_3 \cdot \left({}^{h,l}c_{x,a} \cdot {}^{h,l}H - {}^{h,l}c_{x,g} \right) \text{ (phase exchange column)} \tag{8}$$

242 $$^{l}r_4 = k_4 \cdot \frac{{}^{l}c_{x,a}}{K_s + {}^{l}c_{x,a} + {}^{h}c_{x,a} \cdot \alpha_b} \qquad \text{(degradation non-deuterated toluene)} \tag{9}$$

243 $$^{h}r_4 = k_4 \cdot \alpha_b \cdot \frac{{}^{h}c_{x,a}}{K_s + {}^{l}c_{x,a} + {}^{h}c_{x,a} \cdot \alpha_b} \qquad \text{(degradation deuterated toluene)} \tag{10}$$

244 with subscripts g and a denoting gas phase and liquid (aqueous) phase, respectively.

245 Subscript r refers to the reservoir while x refers a location in the column; $x = 0$: bottom

246 of the column, $x = L$ top of the column. $^{h,l}H$ is the dimensionless Henry volatility, $k_{...}$ are

247 rate parameters, K_s is the Michaelis-Menten constant and α_b is the stable isotope

248 fractionation factor of the degradation reaction. Eq. 6 and 7 describe the mass flux

249 (mass per time) between the different compartments, while Eq. 8 directly describes the

250 concentration change (mass per volume per time) in the gas phase of the column. No

251 further species are considered in the simulations. In particular, no oxygen limitation is

252 considered for the degradation kinetics as preliminary simulations have shown that

253 aerobic conditions are maintained for all parts of the systems throughout the

254 experiments, which is in agreement to the experimental observations of Khan, et al.[4] .

255 The kinetic expressions were implemented into the Biogeochemical Reaction Network

256 Simulator[51-53] using a regular spatial discretization of the column of 0.5 cm. Effective

257   gas phase diffusion coefficients are derived from molecular diffusion coefficients $^{h,l}D_m$

258   and the tortuosity τ of the glass bead packing ($^{h,l}D = {}^{h,l}D_m \cdot \tau$) (note that partitioning

259   effects between gas phase and aqueous phase are explicitly described in the

260   simulations).

261

262   Parameter values used for the simulations (**Table 1**) were either derived directly from

263   the experimental systems or were fitted to match the experimental observations. For this

264   purpose first the control experiments were used to adjust the parameters of the non-

265   reactive processes. Then parameters describing biodegradation were determined using

266   the data from the systems with biodegradation. The target of the parameter estimation

267   was to obtain simultaneously a good match of the total toluene concentrations in the

268   reservoirs and in the columns, and of the slopes of the Rayleigh plots for the reservoirs

269   and the columns. Parameters were varied without using any automated algorithm. All

270   parameters describing transport and reactions are assumed to be constant in space and

271   time. Exceptions are the water saturation of the columns which is assumed to decrease

272   linearly from initially 14% to 7% after 7 days reflecting the experimental observations

273   (note that this also affects the gas phase volume in the column and that is it assumed

274   that no concentration changes are directly induced by the volume changes due to the fast

275   relaxation of the system compared to the time scale of the volume changes) and k_4

276   (maximum rate of the degradation reaction) which is considered to decrease according

277   to $k_4(t) = k_4(t = 0) \cdot \exp(-\lambda \cdot t)$. Reasons for this decrease in reactivity are not

278   apparent from the experimental data, but the decrease might have been caused by the

279   decreasing water content or a depletion of some trace nutrients. If not stated otherwise

280   parameter values do not differ between the different column reactors, i.e. the presented

281   parameter values describe simultaneously all column reactors. Initial concentrations

282   were set to 0 in the entire systems except of in the liquid phase of the reservoir where

283   concentration values were adjusted to match experimental observations.

RESULTS AND DISCUSSION

Vapor-phase hydrogen stable isotope fractionation in batch reactors

Vapor-phase toluene biodegradation was studied in the batch systems containing deuterated and non-deuterated toluene to obtain the hydrogen stable isotope fractionation factor of toluene by *Pseudomonas putida* KT2442 DsRed pWW0 gfp. All batch reactors exhibited a similar behavior showing a strong hydrogen stable isotope fractionation due to biodegradation (**SI, Figure S3**) with slopes of the Rayleigh plots ranging between -0.86 and -0.97; i.e. stable isotope fractionation factors in the range of 0.03 to 0.14. An additional replicate for Day 1 yielded unreasonable results and was omitted from further analysis. No temporal shifts in fractionation of vapor-phase toluene was observed and the average stable isotope fractionation factor was $\alpha_b = 0.08 \pm 0.05$. This value obtained from vapor-phase toluene data is similar to values reported in Kampara, et al.[45] ($\alpha_b = 0.07 \pm 0.02$) and Morasch, et al.[54] ($\alpha_b = 0.09 \pm 0.07$) for liquid batch systems where fully deuterated toluene was degraded by a closely related bacterial strain having the same TOL plasmid as *P. putida* KT2442. In general, phase transitions may contribute to the stable isotope fractionation in a system.[55-56] The similarity between the results from the two phase system and those reported for the liquid systems suggests that the transition between gas phase and liquid/agar phase did not have any impact on the magnitude of the observable fractionation effects in this study or that any possible effects were in the order of the uncertainties of the measurements.

Hydrogen stable isotope fractionation in column reactors

Control experiments: Results of the two control column reactors showed continuous yet moderate depletion (approx. *10 mgL^{-1}* throughout the experimental period) of toluene in the liquid reservoirs attributed to the losses by diffusion through the column reactors (**SI, Figure S4**). Compared to the strong fractionation observed in the batch reactors (see above), only minor fractionation effects (slopes of the Rayleigh plots of -0.010 to -0.006) were observed in the reservoir indicating that fractionation effects caused by the diffusive transport and or the phase exchange between liquid reservoir and head space are relatively small. In the absence of an isotopoloue-specific Henry's law constant and any effects (masking of fractionation or causing additional fractionation) due to the mass transfer from liquid to water fractionation in the reservoir should be given by α_d,[29]

which is in agreement with the measured data given the rather strong signal to noise ratios. The gas to liquid concentration ratios between liquid reservoir and its headspace were nearly constant during the experiment (**SI, Figure S5**). Along the columns of the control systems, linear concentration profiles were observed indicating quasi-steady state conditions of the diffusive transport (**SI, Figures S6 and S7**). This is in agreement with the approximate relaxation time (time approximately needed to establish steady state conditions) $t_r = L^2/D \approx 8$ h of the diffusion along the column, which is comparably small to the time scale of concentration changes in the reservoir. At steady state, differences in the diffusion coefficients between the two isotopologues would not lead to any fractionation along the column as the steady-state linear concentration profiles are not affected by the values of the diffusion coefficients.[29] This is in agreement with the negligible fractionation effects (trends in the Rayleigh plots rather reflecting the noise level of the measurements) observed along the control reactor columns considered to be at (quasi-)steady state.

The behavior of the control reactors was well captured by the numerical model (**SI, Figures S4-S7**) with the simulated results matching the measured concentrations as well as stable isotope signatures in the reservoir and in the columns. Parameters describing the diffusive transport (**Table 1**) are taken directly from the experimental setup or from the literature, indicating that the model represents a valid conceptualization of the experimental system and that the description of the abiotic processes provides a reliable basis for the simulation of the reactive processes.

Biodegradation experiments – experimental observations: Measured changes in concentrations in the reservoirs of the biodegradation reactors show a decrease in total toluene over an experimental period of seven days (**Figure 1**) which is stronger than observed for the control systems. Column 1 and Column 2 where operated as replicates and exhibit very similar results while Column 3 was operated with a higher initial concentration (approx. *35 mg L⁻¹* vs. *55 mg L⁻¹*) to test the behavior of the setup under different conditions. In contrast to the control systems (**SI, Figure S3**) all bioreactive systems showed pronounced hydrogen stable isotope fractionation with slopes of the Rayleigh plots in the range of -0.3 for Column 1 and Column 2 and -0.5 for Column 3 (**Figure 1**). This indicates biodegradation leading to higher losses of toluene to the unsaturated part of the system Khan, et al.[4] and that the fractionation caused by the biodegradation leading to enrichment of the heavy isotopes in the liquid reservoir

351 representing the source zone of the VOC as previously reported by Bouchard, et al.[29] As

352 already discussed in Khan, et al.[4] the increase of the gas to liquid concentration ratios in

353 the reservoir during the course of the experiment (from approx. 0.1 to 0.3; **Figure 2**)

354 indicates a rate limiting effect of the phase exchange from liquid reservoir to its head

355 space for the entire losses of toluene from the system. This is further confirmed by

356 comparing measured slopes of the Rayleigh plots with predictions of the 'source

357 fractionation factor' by Bouchard et al.[44] When neglecting finite-size effects of the

358 column and isotopologue-specific Henry's law constants the source fractionation factor

359 should be equal to $\sqrt{\alpha_b \cdot \alpha_d}$ with α_d derived from **Table 1** and α_b as determined from

360 the batch experiments, the slopes of the Rayleigh plots for the reservoirs should be -

361 0.719 ± 0.088. The observed differences between predicted and measured values

362 indicate a masking of the fractionation in the reservoir due to the rate-limiting phase

363 exchange. Concentration profiles along the columns of the bioreactive systems observed

364 at (quasi-)steady-state conditions at two different observation days clearly deviate from

365 the linear profiles observed for the control systems, which confirms biodegradation to

366 have taken place. This was associated with strong hydrogen stable isotope fractionation

367 along the columns (**Figures 3 and 4**). For Column 1 the slopes of the Rayleigh plots

368 were in the range of -0.55 to -0.6 and for Column 2 and Column 3 slopes were in the

369 range of -0.7 and below. While these slopes indicated a strong fractionation due to

370 biodegradation, their values are higher (less negative) than the slopes observed for the

371 batch reactor systems. This is in agreement with the analytical calculations predicting

372 slopes to be controlled by $\sqrt{\alpha_b}$ rather than by α_b as in the batch experiments, see Eq. 5.

373 Using Eq. 5, with α_d again derived from **Table 1** and α_b as determined from the batch

374 experiments, the slopes of the Rayleigh plots for the columns should be -0.716 ± 0.089

375 which covers the observed values for Column 2 and Column 3. Slopes for Column 1

376 were slightly below this range which indicates for this system a possible masking of the

377 stable isotope fractionation, e.g. due to mass transfer limitations.[37, 45, 57]

378

379 ***Biodegradation experiments - numerical simulations:*** Results of the simulations

380 allowed for a good fit between simulated and experimental data (**Figures 1-4**). Both,

381 concentration changes and stable isotope fractionation were well described with the

382 used modeling concept. Values of the fitting parameters (**Table 1**) were adjusted in a

383 non-automated procedure and are in good agreement with literature values (for the

384   Henry volatilities) or predictions from boundary layer theories (time constants for phase
385   exchange). In particular, for the fractionation factor of the biodegradation reaction the
386   value of $\alpha_b = 0.05$ obtained by the model fitting coincided well with the observed range
387   of 0.08 ± 0.05 obtained in the batch experiments. Furthermore, this suggests that the
388   model was able to provide a valid description of the reactive transformations in the
389   column reactors. The simulation results also showed that the microbial reactivity of the
390   columns decreased over time as is likely to be explained by a gradual exhaustion of
391   nutrients during the course of the experiments. Simulation results also show that
392   although the three biodegradation columns performed similarly their initial reactivity
393   varied by a factor of up to 4 (**Table 1**). As the columns were all inoculated similarly,
394   these variations might be caused by random/natural variations of microbial abundance
395   and activity in the inoculum. The simulation results confirm that isotope fractionation in
396   the reservoirs was masked by a rate-limiting phase exchange between the liquid
397   reservoir and its headspace an observation made for several mass-transfer limited
398   systems [14]. The same limitation is also the reason for the disequilibrium of gas to liquid
399   concentration ratios in the reservoirs (**Figure 2**) confirming previous interpretations of
400   the experimental results.
401
402   ***Factors affecting isotope fractionation of vapor-phase toluene during diffusive***
403   ***transport in column experiments***
404   ***General considerations:*** The slopes of the Rayleigh plots obtained from the studied
405   columns do not match the fractionation factors of the microbial degradation reaction
406   observed in the batch reactors. This was expected giving the diffusion-dominated
407   transport regime in the column reactors. Both, experimental observation and simulation
408   results also reveal that the slopes show a deviation from the predictions of $m = -0.775$
409   provided by Eq. 5 (using the fitted value for α_b) with strongest deviations observed for
410   the reactor Column 1. As will be discussed below, potential reasons for this behavior
411   are two inherent assumptions in Eq. 5 that are not met in the column reactors: the
412   column length was not infinitely long and the degradation was not following first order
413   kinetics. If the columns are not well described by a semi-infitite system (see
414   requirement for Eq. 3) finite size effects can lead to less negative slopes of the Rayleigh
415   plot; especially when analyzing data up to the outlet (i.e., the zero concentration end of
416   the column; **SI, Figure S8**). These effects are observed when reaction is slow compared
417   to diffusive transport (i.e. for small Damköhler numbers; $Da < 10^2\text{-}10^3$) or in practical

terms whenever concentrations are not fully depleted well before the zero concentration end. Less negative slopes than predicted by Eq. 5 may also arise if degradation processes follow Michaelis-Menten kinetics instead of first order kinetics (**SI, Figure S9**). Such effects are most pronounced close to the source of the concentration where higher concentrations lead to a stronger deviation from first-order kinetics. Consequently, the higher the source concentration (i.e., the higher the ratio between source concentration and Michelis-Menten constant) the stronger the deviation of the Rayleigh plot slopes from the theoretical prediction. Furthermore, mass transfer limitations inside the column reactor packing may have masked the microbially induced isotope fractionation. Mass transfer related limitations of substrate bioavailability are known to lead to less observable fractionation (i.e. less negative slopes).[14-15, 37, 45, 57] This effect is more pronounced for lower concentrations (i.e. low ratios between concentration and Michaelis-Menten constant) than for higher concentrations.[37] Consequently, each of these effects or any combination of them could be the reason for deviations between observed and predicted slopes of the Rayleigh plots. The dependency of these effects on concentration or distance to the column ends can also lead to changes of the slopes along the diffusive path and thus to a dependency of the obtained slopes on the analyzed data range (**SI, Figures S8 and S9**). Additional transient effects (i.e. deviations from steady state) are not considered due to the short relaxation time of the system compared to the slow gradual changes of reservoir concentrations and microbial reactivity.

Analysis of individual factors – sensitivity analysis: To determine the contribution of each of these processes to the observed fractionation effects and resulting slopes of the Rayleigh plots in the three-bioreactive column reactors a number of additional simulations were made to test the sensitivity of the results to variations of different parameters. Variations include an increase of the column length from 35 cm to 70 cm to test for finite size effects, an increase of the phase exchange time constant between vapor and liquid phase in the columns by different factors to test for bioavailability restrictions and the associated masking of the fractionation, and an increase of the Michaelis-Menten constant and the initial maximum biodegradation rate parameter (both by the same factor) to test for effects from using non-first order kinetics. These variations also lead to (minor to major) changes of the concentration profiles along the column reactors, which challenges the comparison of slopes from different simulations.

452 For the comparison between experimental and simulated results, model data were
453 analyzed for the same column segments for which isotope ratios were measurable in the
454 experiments (i.e. non-deuterated toluene above detection limit). Using these segments
455 for all sensitivity tests lead to different concentration ranges analyzed each time. Thus
456 simulated slopes were additionally analyzed for a range defined by an arbitrary limit of
457 $\ln(R/R_0) = 7$ covering variation of R by approximately three orders of magnitude. An
458 overview of these results is provided in the Supporting Information (**Table S1**). The
459 obtained results show that deviations between observed and predicted slopes could
460 mainly be attributed to mass transfer induced limitations of substrate bioavailability.
461 This effect is most pronounced for reactor Column 1 which had the highest reactivity
462 and least negative slopes. In turn, for reactor Column 3 at day 5 which had the lowest
463 reactivity and high reservoir concentration an increased bioavailability had the least
464 effects on the observed fractionation effects. The lower reactivity and higher
465 concentrations of the latter case also explain why only in this case an increase of the
466 column length had a minor effect on the observed fractionation effect as non-negligible
467 concentration values were found in the vicinity of the zero-concentration boundary (for
468 the original column length). For the other two reactors an increase of the column length
469 had no (or negligible) effects on the slopes of the Rayleigh plots. An analysis of the
470 influence of the degradation kinetics on the slopes was not straightforward as these
471 changes had also a major effect on the concentration profiles. Furthermore, according to
472 Thullner, et al.[37] the substrate bioavailability depends on two quantities: the ratio
473 between concentration and Michaelis-Menten constant and the ratio between the
474 specific affinity and the time constant of the phase-exchange in the columns. While the
475 specific affinity (i.e. the ratio between maximum degradation rate parameter and
476 Michaelis-Menten constant) was kept constant, the ratio between concentrations and
477 Michaelis-Menten constant was not and thus a variation of this parameter led to
478 differing trends depending on the relevance of bioavailability restrictions. Using the
479 $\ln(R/R_0) \leqslant 7$ criterion for comparison showed all in all a rather limited sensitivity of
480 the slopes to the choice of reaction kinetics: Those data sets showing highest influence
481 of bioavailability restrictions (Column 1 and Column 2, day 2) exhibited slightly less
482 negative slopes if the reaction kinetics became closer to first-order kinetics, while the
483 other data set exhibited slightly more negative slopes. The only exception was again
484 found for reaction Column 3 (day 5) where initial concentrations were higher and thus
485 degradation kinetics differing more from first order. To isolate effects from the used

486 reaction kinetics in a better way simulations were also performed combining conditions
487 with no bioavailability restrictions (i.e. high phase-exchange time constant) with an
488 increased value of the Michaelis-Menten constant. High bioavailability and increased
489 column length led to slopes deviating only up to 0.030 (using the $\ln(R/R_0) \leqslant 7$ criterion
490 for comparison) from the theoretically expected value of -0.775. A shift of the
491 degradation kinetics toward first-order kinetics decreased this deviation to 0.009 or less.
492 In summary, the performed sensitivity analysis showed that all three tested factors had
493 some influence on the slopes of the Rayleigh plots along the column reactors. The most
494 significant factor was the limitation of bioavailability while the other two factors had
495 only minor to negligible effects on the slopes. All tested factors led to less negative
496 slopes than theoretically predicted, which in turn means that using Eq. 5 for converting
497 an experimentally determined slope of a Rayleigh plot into and apparent stable isotope
498 fractionation factor would lead to an overestimation of the fractionation factor (i.e.,
499 estimated values of α_b are closer to 1). However, estimation errors are in the same range
500 as experimental uncertainties in measuring fractionation factors.
501
502 *Implications for other studies*
503 Our findings reflect that compound-specific stable isotope analysis can be a tool for
504 quantitative as well as qualitative estimates of the major subsurface processes in
505 diffusion-dominated systems. This enlarges the range of application of CSIA for the
506 assessment of (contaminant) biodegration in the subsurface. In spite of the contribution
507 of diffusive mixing and diffusion induced fractionation,[28] our results show that the
508 magnitude of isotope fractionation due to biodegradation can be quantitatively
509 estimated if concentration gradients have approximately achieved a steady-state. The
510 application of the presented concepts is not limited to the high stable isotope
511 fractionation factor associated with the biodegradation but may also be used for
512 conditions encountered in real world systems as neither the basic principles nor the
513 computational procedures depend on the magnitude of the fractionation factors or the
514 relative abundance of the different isotopologues. Biodegradation of VOC in the
515 unsaturated subsurface can mitigate emissions of contaminants to the atmosphere[2-3, 35, 58]
516 or may reduce the chance of vapor-phase intrusion into buildings.[59-61] An assessment of
517 such degradation *in situ* is possible using concentration data[50] yet it is challenging given
518 the problems associated obtaining a sufficient number of *in-situ* samples. The presented
519 concepts allow using CSIA as an additional and highly beneficial source of information

520   for an existing number of samples even if diffusion is the dominant transport process.

521   Furthermore our results confirm that in cases where the stable isotope fractionation

522   factors of the biodegradation reaction are close to those of diffusion a lack of

523   fractionation along a diffusive flow path (as has been observed for systems with proven

524   biodegradation when approaching steady state[29, 44]) is not necessarily an indication for

525   the absence of biodegradation.

526

527 # ASSOCIATED CONTENT

528 **Supporting Information**

529 The supporting Information is available free of charge on the ACS Publications website
530 at DOI: xxxxxxxxxxxxxx

531 Descriptions of the batch systems, bioreactive columns and modeling approach
532 used to interpret the results. Along with results from the control systems.

533

534 # AUTHOR INFORMATION

535 **Corresponding Author**

536 *Phone: +49 3412351338. Email: martin.thullner@ufz.de

537 **ORCID**

538 Ali M. Khan: 0000-0002-0253-1169

539 Lukas Y Wick: 0000-0001-7296-865X

540 Martin Thullner: 0000-0001-9723-4601

541 **Notes**

542 The authors declare no competing financial interest.

543

ACKNOWLEDGMENTS

REFERENCES

1.   Bouchard, D.; Hunkeler, D.; Gaganis, P.; Aravena, R.; Höhener, P.; Broholm, M. M.; Kjeldsen, P., Carbon isotope fractionation during diffusion and biodegradation of petroleum hydrocarbons in the unsaturated zone: Field experiment at Vaerlose airbase, Denmark, and modeling. *Environ. Sci. Technol.Environ. Sci. Technol.Environ. Sci. Technol.* **2008,** *42* (2), 596-601.

2.   De Biase, C.; Reger, D.; Schmidt, A.; Jechalke, S.; Reiche, N.; Martinez-Lavanchy, P. M.; Rosell, M.; Van Afferden, M.; Maier, U.; Oswald, S. E.; Thullner, M., Treatment of volatile organic contaminants in a vertical flow filter: Relevance of different removal processes. *Ecological Engineering* **2011,** *37* (9), 1292-1303.

3.   van Afferden, M.; Rahman, K. Z.; Mosig, P.; De Biase, C.; Thullner, M.; Oswald, S. E.; Muller, R. A., Remediation of groundwater contaminated with MTBE and benzene: The potential of vertical-flow soil filter systems. *Water Res.* **2011,** *45* (16), 5063-5074.

4.   Khan, A. M.; Wick, L. Y.; Harms, H.; Thullner, M., Biodegradation of vapor-phase toluene in unsaturated porous media: Column experiments. *Environmental Pollution* **2016,** *211*, 325-31.

5.   Meckenstock, R. U.; Morasch, B.; Griebler, C.; Richnow, H. H., Stable isotope fractionation analysis as a tool to monitor biodegradation in contaminated acquifers. *J. Contam. Hydrol.* **2004,** *75* (3-4), 215-55.

6.   Schmidt, T. C.; Zwank, L.; Elsner, M.; Berg, M.; Meckenstock, R. U.; Haderlein, S. B., Compound-specific stable isotope analysis of organic contaminants in natural environments: a critical review of the state of the art, prospects, and future challenges. *Anal. Bioanal. Chem.* **2004,** *378* (2), 283-300.

7.   Elsner, M., Stable isotope fractionation to investigate natural transformation mechanisms of organic contaminants: principles, prospects and limitations. *J. Environ. Monit.* **2010,** *12* (11), 2005-2031.

8.   Thullner, M.; Centler, F.; Richnow, H.-H.; Fischer, A., Quantification of organic pollutant degradation in contaminated aquifers using compound specific stable isotope analysis – Review of recent developments. *Org. Geochem.* **2012,** *42* (12), 1440-1460.

9.   Fischer, A.; Theuerkorn, K.; Stelzer, N.; Gehre, M.; Thullner, M.; Richnow, H. H., Applicability of stable isotope fractionation analysis for the characterization of benzene biodegradation in a BTEX-contaminated aquifer. *Environ. Sci. Technol.* **2007,** *41* (10), 3689-3696.

10.   Druhan, J. L.; Maher, K., The influence of mixing on stable isotope ratios in porous media: A revised Rayleigh model. *Water Resour. Res.* **2017,** *53*, 1101-1124.

593 11.   Harrington, R. R.; Poulson, S. R.; Drever, J. I.; Colberg, P. J. S.; Kelly, E. F., Carbon
594 isotope systematics of monoaromatic hydrocarbons: vaporization and adsorption
595 experiments. *Org. Geochem.* **1999,** *30* (8A), 765-775.

596 12.   Schüth, C.; Taubald, H.; Bolano, N.; Maciejczyk, K., Carbon and hydrogen
597 isotope effects during sorption of organic contaminants on carbonaceous materials. *J.
598 Contam. Hydrol.* **2003,** *64* (3-4), 269-281.

599 13.   Kopinke, F. D.; Georgi, A.; Voskamp, M.; Richnow, H. H., Carbon isotope
600 fractionation of organic contaminants due to retardation on humic substances:
601 Implications for natural attenuation studies in aquifers. *Environ. Sci. Technol.Environ.
602 Sci. Technol.* **2005,** *39* (16), 6052-6062.

603 14.   Thullner, M.; Fischer, A.; Richnow, H. H.; Wick, L. Y., Influence of mass transfer
604 on stable isotope fractionation. *Appl. Microbiol. Biotechnol.* **2013,** *97* (2), 441-452.

605 15.   Heße, F.; Prykhodko, V.; Attinger, S.; Thullner, M., Assessment of the impact of
606 pore-scale mass-transfer restrictions on microbially-induced stable-isotope
607 fractionation.Adv. Water Resour. **2014,** *74*, 79-90.

608 16.   Abe, Y.; Hunkeler, D., Does the Rayleigh equation apply to evaluate field
609 isotope data in contaminant hydrogeology? *Environ. Sci. Technol.Environ. Sci. Technol.*
610 **2006,** *40* (5), 1588-1596.

611 17.   Rolle, M.; Chiogna, G.; Bauer, R.; Griebler, C.; Grathwohl, P., Isotopic
612 Fractionation by Transverse Dispersion: Flow-through Microcosms and Reactive
613 Transport Modeling Study. *Environ. Sci. Technol.Environ. Sci. Technol.* **2010,** *44* (16),
614 6167-6173.

615 18.   Eckert, D.; Rolle, M.; Cirpka, O. A., Numerical simulation of isotope
616 fractionation in steady-state bioreactive transport controlled by transverse mixing. *J.
617 Contam. Hydrol.* **2012,** *140-141*, 95-106.

618 19.   Maggi, F.; Riley, W. J., Transient competitive complexation in biological kinetic
619 isotope fractionation explains nonsteady isotopic effects: Theory and application to
620 denitrification in soils. *J. Geophys. Res.* **2009,** *114* (G4).

621 20.   Rayleigh, L., L.Theoretical considerations respecting the separation of gases by
622 diffusion and similar processes. *Philosophical Magazine Series 5* **1896,** *42* (259), 493-
623 498.

624 21.   Mariotti, A.; Germon, J. C.; Hubert, P.; Kaiser, P.; Letolle, R.; Tardieux, A.;
625 Tardieux, P., Experimental Determination of Nitrogen Kintic Isotope Fractionation:
626 Some Priciples; Illustration for the Denitrification and Nitrification Processes. *Plant Soil*
627 **1981,** *62* (3), 413-430.

628 22.   Richnow, H. H.; Annweiler, E.; Michaelis, W.; Meckenstock, R. U., Microbial in
629 situ degradation of aromatic hydrocarbons in a contaminated aquifer monitored by
630 carbon isotope fractionation. *J. Contam. Hydrol.* **2003,** *65* (1-2), 101-120.

631   23.   Hunkeler, D.; Meckenstock, R. U.; Sherwood Lollar, B.; Schmidt, T. C.; Wilson, J.
632 T. *A Guide for Assessing Biodegradation and Source Identification of Organic Ground*
633 *Water Contaminants using Compound Specific Isotope Analysis (CSIA)*; EPA 600/R-
634 08/148; EPA, United States Environmental Protection Agency, Office of Research and
635 Development, National Risk Management Research Laboratory, Arda OK, USA: 2008.

636   24.   Fuller, E. N.; Schettler, P. D.; Giddings, J. C., A new method for prediction of
637 binary gas-phase diffusion coefficients. *Ind. Eng. Chem.* **1966,** *58*, 18-27.

638   25.   Cerling, T. E.; Solomon, D. K.; Quade, J.; Bowman, J. R., On the isotopic
639 composition of carbon in soil carbon dioxide. *Geochim. Cosmochim. Acta* **1991,** *55*,
640 3403-3405.

641   26.   Jin, B.; Rolle, M.; Li, T.; Haderlein, S. B., Diffusive fractionation of BTEX and
642 chlorinated ethenes in aqueous solution: quantification of spatial isotope gradients.
643 *Environ. Sci. Technol.Environ. Sci. Technol.* **2014,** *48* (11), 6141-6150.

644   27.   Wanner, P.; Hunkeler, D., Carbon and chlorine isotopologue fractionation of
645 chlorinated hydrocarbons during diffusion in water and low permeability sediments.
646 *Geochim. Cosmochim. Acta* **2015,** *157*, 198-212.

647   28.   Rolle, M.; Jin, B., Normal and Inverse Diffusive Isotope Fractionation of
648 Deuterated Toluene and Benzene in Aqueous Systems. *Environ. Sci. Technol. Lett.*
649 **2017,** *4* (7), 298-304.

650   29.   Bouchard, D.; Höhener, P.; Hunkeler, D., Carbon Isotope Fractionation During
651 Volatilization of Petroleum Hydrocarbons and Diffusion Across a Porous Medium: A
652 Column Experiment. *Environ. Sci. Technol.* **2008,** *42* (21), 7801-7806.

653   30.   Dale, A. W.; Brüchert, V.; Alperin, M.; Regnier, P., An integrated sulfur isotope
654 model for Namibian shelf sediments. *Geochim. Cosmochim. Acta* **2009,** *73* (7), 1924-
655 1944.

656   31.   Jeannottat, S.; Hunkeler, D., Chlorine and carbon isotopes fractionation during
657 volatilization and diffusive transport of trichloroethene in the unsaturated zone.
658 *Environ. Sci. Technol.* **2012,** *46* (6), 3169-76.

659   32.   Cerling, T. E., The stable isotopic composition of modern soil carbonate and its
660 relationship to climate. *Earth Planet. Sci. Lett.* **1984,** *71*, 229-240.

661   33.   Barry, D. A.; Prommer, H.; Miller, C. T.; Engesgaard, P.; Brun, A.; Zheng, C.,
662 Modelling the fate of oxidisable organic contaminants in groundwater.Adv. Water
663 Resour. **2002,** *25* (8-12), 945-983.

664   34.   Molins, S.; Mayer, K. U.; Amos, R. T.; Bekins, B. A., Vadose zone attenuation of
665 organic compounds at a crude oil spill site - interactions between biogeochemical
666 reactions and multicomponent gas transport. *J. Contam. Hydrol.* **2010,** *112* (1-4), 15-
667 29.

668　35.　De Biase, C.; Carminati, A.; Oswald, S. E.; Thullner, M., Numerical modeling
669　analysis of VOC removal processes in different aerobic vertical flow systems for
670　groundwater remediation. *J. Contam. Hydrol.* **2013,** *154*, 53-69.

671　36.　van Breukelen, B. M.; Griffioen, J.; Roling, W. F. M.; van Verseveld, H. W.,
672　Reactive transport modelling of biogeochemical processes and carbon isotope
673　geochemistry inside a landfill leachate plume. *J. Contam. Hydrol.* **2004,** *70* (3-4), 249-
674　269.

675　37.　Thullner, M.; Kampara, M.; Richnow, H. H.; Harms, H.; Wick, L. Y., Impact of
676　bioavailability restrictions on microbially induced stable isotope fractionation. 1.
677　Theoretical calculation. *Environ. Sci. Technol.* **2008,** *42* (17), 6544-6551.

678　38.　Hunkeler, D.; Van Breukelen, B. M.; Elsner, M., Modeling Chlorine Isotope
679　Trends during Sequential Transformation of Chlorinated Ethenes. *Environ. Sci. Technol.*
680　**2009,** *43* (17), 6750-6756.

681　39.　Prommer, H.; Anneser, B.; Rolle, M.; Einsiedl, F.; Griebler, C., Biogeochemical
682　and Isotopic Gradients in a BTEX/PAH Contaminant Plume: Model-Based Interpretation
683　of a High-Resolution Field Data Set. *Environ. Sci. Technol.* **2009,** *43* (21), 8206-8212.

684　40.　Centler, F.; Hesse, F.; Thullner, M., Estimating pathway-specific contributions to
685　biodegradation in aquifers based on dual isotope analysis: Theoretical analysis and
686　reactive transport simulations. *J. Contam. Hydrol.* **2013,** *152C*, 97-116.

687　41.　Eckert, D.; Qiu, S.; Elsner, M.; Cirpka, O. A., Model complexity needed for
688　quantitative analysis of high resolution isotope and concentration data from a toluene-
689　pulse experiment. *Environ. Sci. Technol.* **2013,** *47* (13), 6900-6907.

690　42.　Druhan, J. L.; Steefel, C. I.; Conrad, M. E.; DePaolo, D. J., A large column analog
691　experiment of stable isotope variations during reactive transport: I. A comprehensive
692　model of sulfur cycling and δ34S fractionation. *Geochim. Cosmochim. Acta* **2014,** *124*,
693　366-393.

694　43.　Alvarez-Zaldívar, P.; Centler, F.; Maier, U.; Thullner, M.; Imfeld, G.,
695　Biogeochemical modelling of in situ biodegradation and stable isotope fractionation of
696　intermediate chloroethenes in a horizontal subsurface flow wetland. *Ecological*
697　*Engineering* **2016,** *90*, 170-179.

698　44.　Bouchard, D.; Cornaton, F.; Höhener, P.; Hunkeler, D., Analytical modelling of
699　stable isotope fractionation of volatile organic compounds in the unsaturated zone. *J.*
700　*Contam. Hydrol.* **2011,** *119* (1-4), 44-54.

701　45.　Kampara, M.; Thullner, M.; Richnow, H. H.; Harms, H.; Wick, L. Y., Impact of
702　bioavailability restrictions on microbially induced stable isotope fractionation. 2.
703　Experimental evidence. *Environ. Sci. Technol.* **2008,** *42* (17), 6552-6558.

704　46.　Mader, B. T.; Goss, K. U.; J., E. S., Sorption of nonionic, hydrophobic organic
705　chemials to mineral surfaces. *Environ. Sci. Technol.* **1997,** *31*, 1079-1086.

706 47.   Hunkeler, D., Quantification of isotope fractionation in experiments with
707 deuterium-labeled substrate. *Appl. Environ. Microbiol.* **2002,** *68* (10), 5205-5206.

708 48.   Meckenstock, R. U.; Morasch, B.; Griebler, C.; Richnow, H. H., Stable isotope
709 fractionation analysis as a tool to monitor biodegradation in contaminated acquifers. *J.*
710 *Contam. Hydrol.* **2004,** *75* (3-4), 215-255.

711 49.   Wilson, D. J., Soil Gas Volatile Organic Compound Concentration Contours for
712 Locating Vadose Zone Nonaqueous Phase Liquid Contamination. *Environ. Monit.*
713 *Assess.* **1997,** *48*, 73-100.

714 50.   Pasteris, G.; Werner, D.; Kaufmann, K.; Höhener, P., Vapor Phase Transport and
715 Biodegradation of Volatile Fuel Compounds in the Unsaturated Zone: A Large Scale
716 Lysimeter Experiment. *Environ. Sci. Technol.* **2002,** *36* (1), 30-39.

717 51.   Regnier, P.; O'Kane, J. P.; Steefel, C. I.; Vanderborght, J. P., Modeling complex
718 multi-component reactive-transport systems: Towards a simulation environment
719 based on the concept of a Knowledge Base. *Appl. Math. Modeling* **2002,** *26*, 913–927.

720 52.   Thullner, M.; Cappellen, P. V.; Regnier, P., Modeling the impact of microbial
721 activity on redox dynamics in porous media. *Geochim. Cosmochim. Acta,* **2005,** *69*,
722 5005–5019.

723 53.   Centler, F.; Shao, H.; De Biase, C.; Park, C.-H.; Regnier, P.; Kolditz, O.; Thullner,
724 M., GeoSysBRNS—A flexible multidimensional reactive transport model for simulating
725 biogeochemical subsurface processes. *Comput. Geosci.* **2010,** *36* (3), 397-405.

726 54.   Morasch, B.; Richnow, H. H.; Schink, B.; Meckenstock, R. U., Stable hydrogen
727 and carbon isotope fractionation during microbial toluene degradation: Mechanistic
728 and environmental aspects. *Appl. Environ. Microbiol.* **2001,** *67* (10), 4842-4849.

729 55.   Jeannottat, S.; Hunkeler, D., Can soil gas VOCs be related to groundwater
730 plumes based on their isotope signature? *Environ. Sci. Technol.* **2013,** *47* (21), 12115-
731 22.

732 56.   Kuder, T.; Philp, P.; Allen, J., Effects of Volatilization on Carbon and Hydrogen
733 Isotope Ratios of MTBE. *Environ. Sci. Technol.* **2009,** *43* (6), 1763-1768.

734 57.   Kampara, M.; Thullner, M.; Harms, H.; Wick, L. Y., Impact of cell density on
735 microbially induced stable isotope fractionation. *Appl. Microbiol. Biotechnol.* **2009,** *81*
736 (5), 977-985.

737 58.   De Biase, C.; Maier, U.; Baeder-Bederski, O.; Bayer, P.; Oswald, S. E.; Thullner,
738 M., Removal of Volatile Organic Compounds in Vertical Flow Filters: Predictions from
739 Reactive Transport Modeling. *Groundwater Monit. Rem.* **2012,** *32* (2), 106-121.

740 59.   Picone, S.; Valstar, J.; van Gaans, P.; Grotenhuis, T.; Rijnaarts, H., Sensitivity
741 analysis on parameters and processes affecting vapor intrusion risk. *Environ. Toxicol.*
742 *Chem.* **2012,** *31* (5), 1042-52.

743   60.   Swartjes, F. A., Human health risk assessment related to contaminated land: 744   state of the art. *Environ. Geochem. Health* **2015,** *37* (4), 651-73.

745   61.   Parker, T.; White, H.; Taylor, G.; Evans, F.; Pearce, M., Real-world uncertainties 746   during a site assessment of vapour migration into a residential house from soil and 747   groundwater. *Q. J. Eng. Geol. Hydrogeol.* **2017,** *50* (3), 318-332.

748   62.   USEPA   http://www3.epa.gov/ceampubl/learn2model/part- 749   two/onsite/estdiffusion.html [Accessed: 15-11-2015]. (accessed 15/11/2015).

750   63.   Sander, R., Compilation of Henry's law constants (version 4.0) for water as 751   solvent. *Atmos. Chem. Phys.* **2015,** *15* (8), 4399-4981.
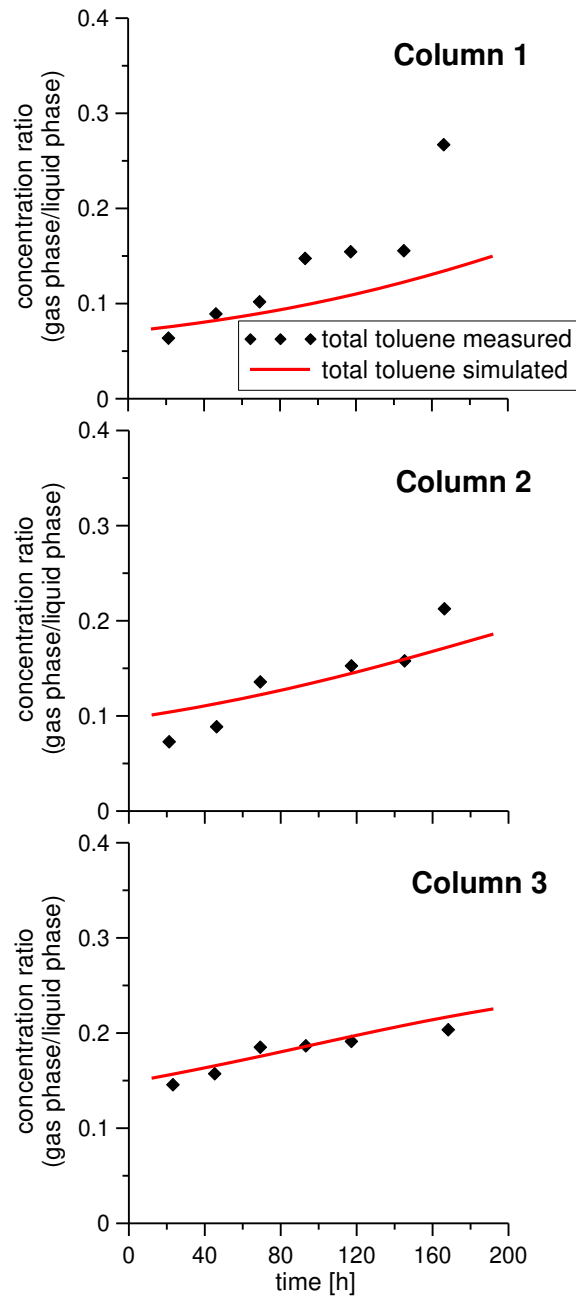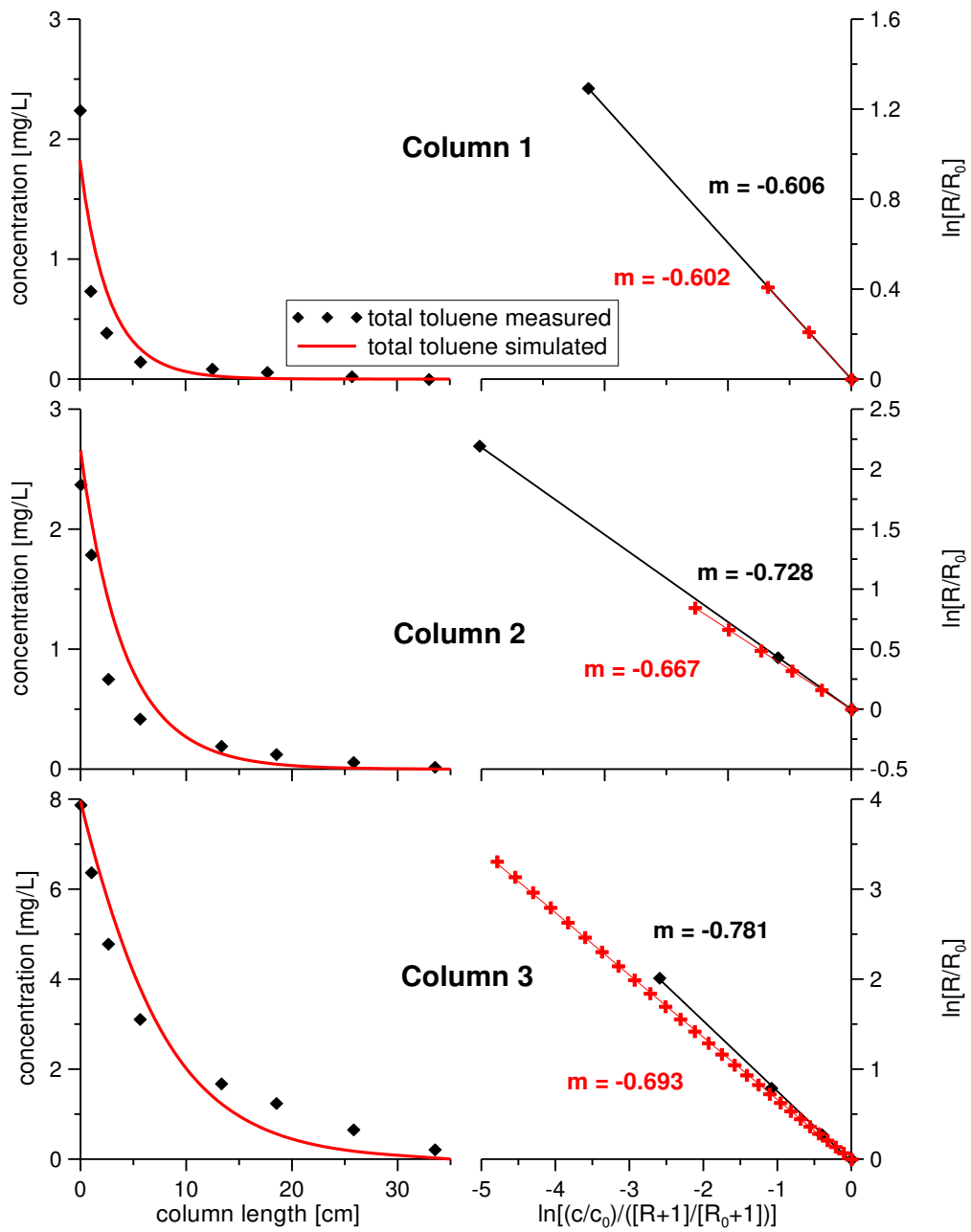752

754

755
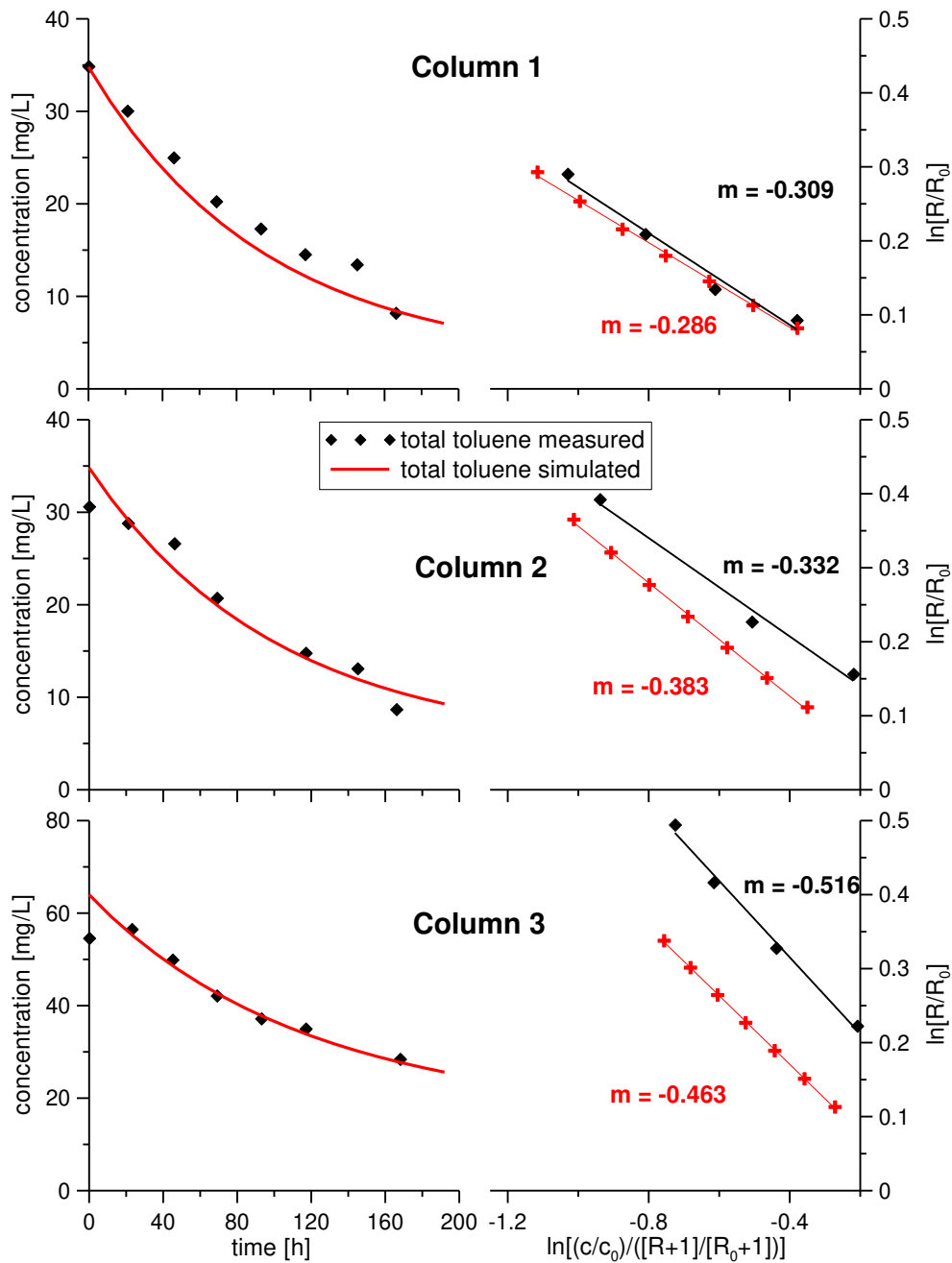
Figure 1: Concentration changes in the liquid reservoirs of the bioreactive column reactors. Symbols mark experimental results, solid lines simulations results. Right: Rayleigh plots of the column reactors. Black diamonds mark experimental results, red crosses mark simulation results at 12-hour intervals. m is the slope of the linear regression fitted to the data.

763

764

765
766
767 **Figure 2:** Gas to liquid concentration ratios in the reservoirs of the bioreactive column
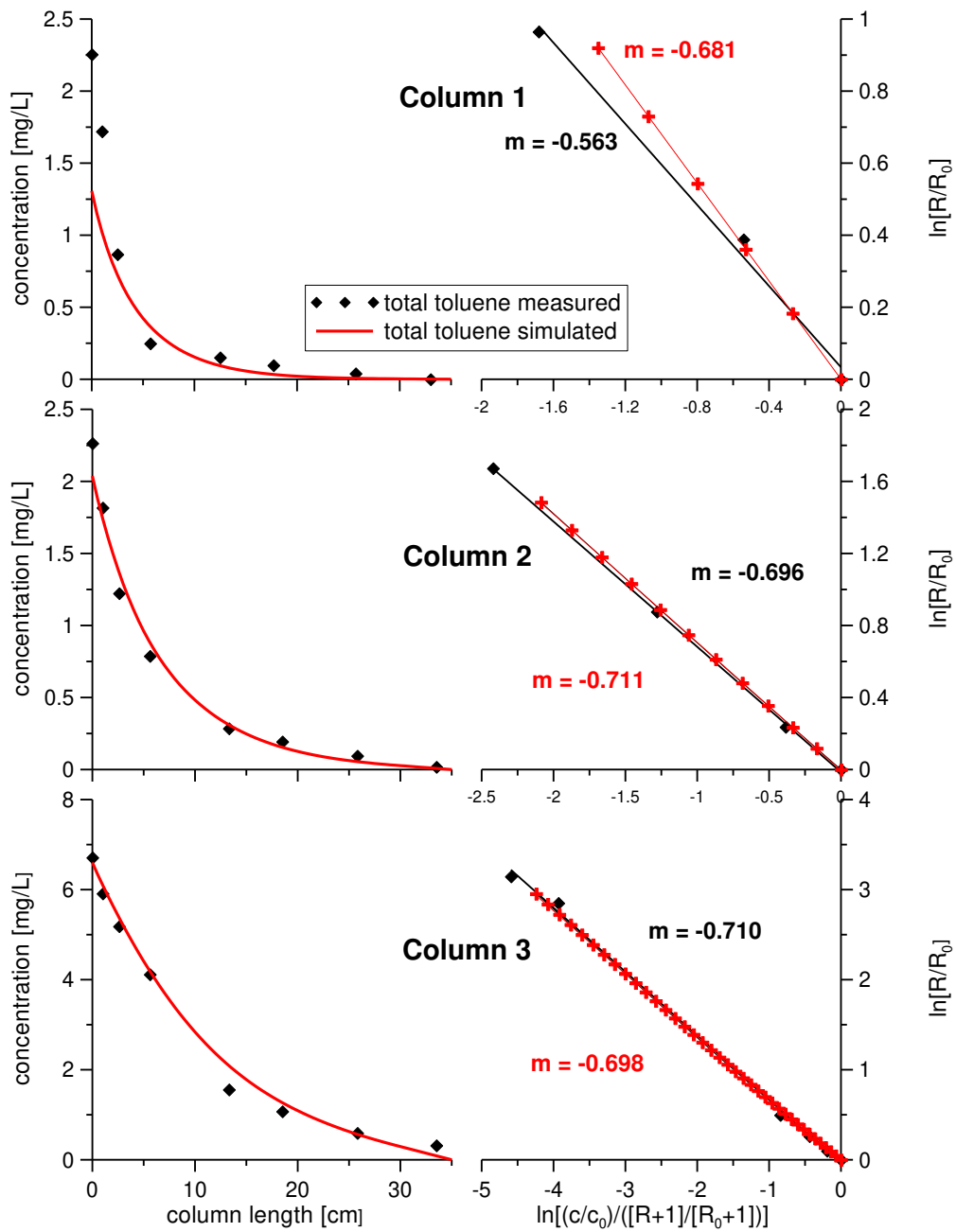768 reactors. Symbols mark experimental results, solid lines simulations results.
769

Figure 3: Left: Concentration profiles along the gas phase of the bioreactive columns after 2 days. Symbols mark experimental results, solid lines simulations results. Right: Rayleigh plots of the bioreactive columns after 2 days. Black diamonds mark experimental results, red crosses mark simulation results. m is the slope of the linear regression fitted to the data.

779

780
781
782 **Figure 4:** Left: Concentration profiles along the gas phase of the bioreactive columns
783 after 5 days. Symbols mark experimental results, solid lines simulations results. Right:
784 Rayleigh plots of the bioreactive columns after 5 days. Black diamonds mark
785 experimental results, red crosses mark simulation results. m is the slope of the linear
786 regression fitted to the data.

787

788

TABLE

790

Table 1: Parameter values used for the numerical simulations.

792

793

Parameter	Description	Value	Origin
L	column length	35 cm	measured
d	column inner diameter	4.1 cm	measured
V_r	reservoir: liquid volume	2375 cm^3	measured
V_h	reservoir: head space volume	45 cm^3	measured
Φ	porosity	0.39	measured
τ	tortuosity	0.5	measured
S	initial water saturation	14%	measured
^hD_m, ^lD_m	gas phase molecular diffusion coefficient	297 cm^2 h^{-1}, 294 cm^2 h^{-1}	USEPA[62] for toluene and modified according to Bouchard, et al.[29] for deuterated toluene
^hH, ^lH	Henry volatility	0.30, 0.30	fitted, constrained by Sander[63]
K_s	Michaelis-Menten constant	0.5 mg L^{-1}	fixed to reasonable value
$^hk_1$, $^lk_1$	time constant for phase exchange in reservoir	100 cm^3 h^{-1}, 100 cm^3 h^{-1}	fitted, constrained by assuming diffusion through liquid boundary layer
$^hk_2$, $^lk_2$	time constant for exchange between head space and column	10^4 cm^3 h^{-1}, 10^4 cm^3 h^{-1}	fixed to high value
$^hk_3$, $^lk_3$	time constant for phase exchange in column	100 h^{-1}, 100 h^{-1}	fitted, constrained by assuming diffusion through liquid boundary layer
k_4	initial maximum rate parameter of biodegradation reaction	552 mg L^{-1} h^{-1} (Column 1) 276 mg L^{-1} h^{-1} (Column 2) 138 mg L^{-1} h^{-1} (Column 3)	fitted
λ	time constant for reactivity decrease	0.01 h^{-1}	fitted
α_b	isotope fractionation factor of biodegradation reaction	0.05	fitted, constrained by batch experiment from this study
$^{h,l}c_i$	initial concentration in reservoir liquid phase	15.5 mg L^{-1} (Control 1) 17.4 mg L^{-1} (Control 2) 17.4 mg L^{-1} (Column 1) 17.4 mg L^{-1} (Column 2) 32.0 mg L^{-1} (Column 3)	adjusted to experimental observations

794

795

796